DMD Fast Forward. Published on November 4, 2019 as DOI: 10.1124/dmd.119.087940
This article has not been copyedited and formatted. The final version may differ from this version.

Title page

Title:

A comparative analysis of cytochrome P450 activities in paired liver and small intestinal samples from patients with obesity

Authors and affiliations:

Veronica Krogstad, Alexandra Peric, Ida Robertsen, Marianne K. Kringen, Christine Wegler, Philip Carlo Angeles, Jøran Hjelmesæth, Cecilia Karlsson, Shalini Andersson, Per Artursson, Anders Åsberg, Tommy B. Andersson, Hege Christensen

Section for Pharmacology and Pharmaceutical Biosciences, Department of Pharmacy, University of Oslo, Oslo, Norway (V.K., I.R., A.Å., H.C.)

Department of Transplantation Medicine, Oslo University Hospital, Rikshospitalet, Oslo, Norway (V.K., A.Å.)

Research and Early Development, Cardiovascular, Renal and Metabolism, BioPharmaceuticals R&D, AstraZeneca Gothenburg, Gothenburg, Sweden (A.P., C.W., S.A., T.B.A.)

Center for Psychopharmacology, Diakonhjemmet Hospital, Oslo, Norway (M.K.K.)

Department of Health Sciences, OsloMet - Oslo Metropolitan University, Oslo, Norway (M.K.K.)

Department of Pharmacy, Uppsala University, Uppsala, Sweden (C.W., P.A.)

The Morbid Obesity Centre, Vestfold Hospital Trust, Tønsberg, Norway (P.C.A., J.H.)

Department of Surgery, Vestfold Hospital Trust, Tønsberg, Norway (P.C.A.)

Department of Endocrinology, Morbid Obesity and Preventive Medicine, Institute of Clinical Medicine, University of Oslo, Oslo, Norway (J.H.)

Late-stage Development, Cardiovascular, Renal and Metabolism, BioPharmaceuticals R&D, AstraZeneca Gothenburg, Gothenburg, Sweden (C.K.)

Department of Molecular and Clinical Medicine, Institute of Medicine, Sahlgrenska Academy, University of Gothenburg, Gothenburg, Sweden (C.K.)

Department of Physiology and Pharmacology, Section of Pharmacogenetics, Karolinska Institutet, Stockholm, Sweden (T.B.A.)

Running title page

Running title:

CYP activities in paired liver and small intestinal samples

Corresponding author:

Veronica Krogstad

Section for Pharmacology and Pharmaceutical Biosciences, Department of Pharmacy, University of Oslo

P.O. Box 1068 Blindern, 0316 Oslo, Norway

Phone: +4791517496

E-mail: veronica.krogstad@farmasi.uio.no

Number of text pages: 29

Number of tables: 8

Number of figures: 6

Number of references: 55

Number of words in Abstract: 247

Number of words in Introduction: 472

Number of words in Discussion: 1497

Abbreviations: ACN, acetonitrile; BMI, body mass index; CL_{int}, intrinsic clearance; CYP, cytochrome P450; fu_{mic}, fraction of unbound drug in microsomes; HIM, human intestinal microsomes; HLM, human liver microsomes; K_m, Michaelis constant; V_{max}, maximum velocity

DMD Fast Forward. Published on November 4, 2019 as DOI: 10.1124/dmd.119.087940
This article has not been copyedited and formatted. The final version may differ from this version.

Abstract

The liver and small intestine restrict oral bioavailability of drugs and constitute the main sites of pharmacokinetic drug-drug interactions. Hence, detailed data on hepatic and intestinal activities of drug metabolizing enzymes is important for modelling drug disposition and optimizing pharmacotherapy in different patient populations. The aim of this study was to determine the activities of seven cytochrome P450 (CYP) enzymes in paired liver and small intestinal samples from patients with obesity. Biopsies were obtained from twenty patients who underwent Roux-en-Y gastric bypass surgery following a three-week low energy diet. Individual hepatic and intestinal microsomes were prepared and specific probe substrates in combined incubations were used for determination of CYP1A2, CYP2B6, CYP2C8, CYP2C9, CYP2C19, CYP2D6 and CYP3A activities. Activities of CYP2C8, CYP2C9, CYP2D6 and CYP3A were quantified in both human liver microsomes (HLM) and human intestinal microsomes (HIM), while activities of CYP1A2, CYP2B6 and CYP2C19 were only quantifiable in HLM. Considerable interindividual variability was present in both HLM (9 to 23-fold) and HIM (5 to 55-fold). The median metabolic HLM/HIM ratios varied from 1.5 for CYP3A to 252 for CYP2C8. Activities of CYP2C9 in paired HLM and HIM were positively correlated ($r=0.74$, $p<0.001$), while no interorgan correlations were found for activities of CYP2C8, CYP2D6 and CYP3A ($p>0.05$). Small intestinal CYP3A activities were higher in females compared with males ($p<0.05$). Hepatic CYP2B6 activity correlated negatively with body mass index ($r=-0.72$, $p<0.001$). These data may be useful for further *in vitro-in vivo* predictions of drug disposition in patients with obesity.

Significance statement

Hepatic and intestinal drug metabolism are key determinants of oral drug bioavailability. In this study, paired liver and jejunum samples were obtained from twenty patients with obesity undergoing gastric bypass surgery following a three-week low energy diet. We determined the hepatic and small intestinal activities of clinically important CYP enzymes and provide detailed enzyme kinetic data relevant for predicting *in vivo* disposition of CYP substrates in this patient population.

DMD Fast Forward. Published on November 4, 2019 as DOI: 10.1124/dmd.119.087940
This article has not been copyedited and formatted. The final version may differ from this version.

Introduction

The liver and small intestine are the primary sites of drug metabolism, influencing both oral bioavailability and clearance and thereby the systemic exposure of drugs. The main group of drug metabolizing enzymes is the cytochromes P450 (CYP) in which the families CYP1-3 are estimated to be responsible for 70-80 % of all phase I drug metabolism (Ingelman-Sundberg, 2005). The CYP3A subfamily, comprising the isoforms CYP3A4 and CYP3A5 in adults, is considered the clinically most important due to its broad substrate specificity. A wide range of drug metabolizing CYP enzymes are expressed in the liver, including CYP1A2, CYP2A6, CYP2B6, CYP2C8, CYP2C9, CYP2C19, CYP2D6, CYP2E1 and CYP3A4/5 (Achour et al., 2014; Shimada et al., 1994). In the small intestine, a more limited number of CYPs are expressed at relevant levels and the CYP3A subfamily is estimated to represent about 80 % of the total intestinal CYP content, followed by CYP2C9 accounting for about 15 % (Paine et al., 2006). Additionally, the hepatic levels of CYP enzymes are considerably higher than in the intestine, and the total small intestinal CYP3A amount has been estimated to equal approximately 1 % of that in the liver (Paine et al., 1997). There is, however, large interindividual variability in the expression and activities of the various CYP isoforms (Achour et al., 2014; Obach et al., 2001; Paine et al., 2006; Yang et al., 2012). This may be partly due to genetic polymorphisms, but other factors such as disease state, dietary constituents and concomitant use of drugs can also affect CYP activity and hence the pharmacokinetics of CYP substrates (Morgan et al., 2008; Shah and Smith, 2015; Zanger and Schwab, 2013).

Obesity, defined by a body mass index (BMI) of 30 kg/m^2 or above, has been associated with altered pharmacokinetics of CYP substrates, but the underlying mechanisms have not been clarified (Brill et al., 2012). As polypharmacy is common due to comorbidities, it is important to gain a more in-depth understanding of interindividual variability in drug metabolizing capacity in this patient group. Physiologically based pharmacokinetic models are important tools for

predicting drug disposition, and in order to perform high quality modelling of oral bioavailability, detailed data on CYP activities at the major sites of drug metabolism, i.e. liver and small intestine, is important. Data on CYP expression and activity in paired human tissue samples is limited (Drozdzik et al., 2017; Lin et al., 2002; Lloret-Linares et al., 2019; Läpple et al., 2003; Paine et al., 1997; Ulvestad et al., 2013; von Richter et al., 2004), and no studies have to the authors knowledge compared hepatic and intestinal activities in patients with obesity. Hence, the aim of this study was to determine the interindividual variability and covariation of microsomal CYP1A2, CYP2B6, CYP2C8, CYP2C9, CYP2C19, CYP2D6 and CYP3A activities in paired liver and small intestinal biopsies from 20 patients with severe obesity.

DMD Fast Forward. Published on November 4, 2019 as DOI: 10.1124/dmd.119.087940
This article has not been copyedited and formatted. The final version may differ from this version.

Materials and methods

Chemicals. Tris base, protease inhibitor cocktail tablets (Complete, Mini), HEPES buffer and reduced β-nicotinamide adenine dinucleotide phosphate (NADPH) were purchased from Sigma-Aldrich (St. Louis, MO). Sucrose and methanol were obtained from Merck (Kenilworth, NJ). Acetonitrile (ACN) was from Fisher Scientific (Waltham, MA). Ethylenediaminetetraacetic acid (EDTA) was purchased from Ferak (Berlin, Germany). Phosphate buffer was prepared from dipotassium hydrogen phosphate and potassium dihydrogen phosphate from Sigma-Aldrich. CYP probe substrates, metabolites and internal standard (5,5-diethyl-1,3-diphenyl-2-iminobarbituric acid) were prepared in-house or obtained from Sigma-Aldrich. High purity water was prepared with a Milli-Q® Water Purification System (Merck).

Patients. Twenty patients (six males and fourteen females) with severe obesity (BMI ≥40 kg/m^2 or 35-40 kg/m^2 combined with at least one obesity-related comorbidity) underwent Roux-en-Y gastric bypass surgery in the COCKTAIL study (trial registration number NCT02386917) (Hjelmesæth et al., 2018). Anthropometric measurements and blood samples for clinical chemistry analyses were collected the day before surgery. Total body weight was determined using the Inbody 720, Body Composition Analyzer (Biospace, Korea). Height was measured to the nearest 1 cm and BMI was calculated as weight in kilograms divided by the square of height in meters. Measurements of waist and hip circumference were standardized and performed by dedicated study personnel. Clinical chemistry analyses were performed at the Department of Laboratory Medicine at Vestfold Hospital Trust. High-sensitivity C-reactive protein was analyzed at Fürst Medical Laboratory (Oslo, Norway). The patients were subjected to a three-week low energy diet (<1200 kcal/day) before surgery. None of the patients received drugs before or during surgery known to alter the activities of the CYP enzymes investigated in the current study. This study complied with the Declaration of Helsinki. The study protocol was approved by the Regional Committee for Medical and Health Research Ethics (2013/2379/REK sørøst A), and all

patients signed a written informed consent. As this was an exploratory study, an a priori power calculation was not performed.

Small intestinal and hepatic biopsies. Paired jejunal and liver biopsies were obtained from each patient during surgery. The distal end of the biliopancreatic limb (proximal jejunum) was resected and removed to allow for biopsy harvesting. Liver tissue was obtained from parenchyma, by cutting a sample close to the edge of the right liver lobe with cold scissors. The tissue samples were transferred into individual cryotubes, snap frozen in liquid nitrogen immediately after sampling and stored at -80 °C until analysis.

Preparation of microsomal fractions. The liver (100 (± 81) mg) and jejunal (687 (± 277) mg) biopsies were thawed on ice and homogenates were prepared with a Potter-Elvehjem homogenizer (5 mL) in buffer containing 0.32 mol/L sucrose, 10 mmol/L Tris base and protease inhibitor cocktail (Complete, Mini, 1 tablet per 10 mL buffer). The homogenization was performed at 2,000 rpm in two rounds of 10 strokes for the jejunum samples and two rounds of 8 strokes for the liver samples. The samples were placed on ice in-between rounds. The homogenate was centrifuged at 7,400 g for 10 minutes (4 °C) and the pellet was discarded. The supernatant was centrifuged at 104,000 g for 60 minutes (4 °C), and the microsomal pellet was resuspended in buffer containing 0.25 mol/L sucrose, 10 mmol/L hepes buffer and 2 mmol/L EDTA. The microsomes were stored at -80 °C until CYP activity analysis. A small volume (10 µL) was stored separately for determination of microsomal protein concentration (BioRad protein assay, based on the Bradford dye-binding method) (Bradford, 1976).

Probe substrates. Specific probe substrates in combined incubations were used for studying the activities of the seven CYP enzymes; bupropion (CYP2B6), amodiaquine (CYP2C8), diclofenac (CYP2C9), bufuralol (CYP2D6), midazolam (CYP3A), phenacetin (CYP1A2) and S-mephenytoin (CYP2C19) (Table 1) (Spaggiari et al., 2014). The probe substrates were divided into two cocktails to minimize interactions (unpublished data, Table 1).

DMD Fast Forward. Published on November 4, 2019 as DOI: 10.1124/dmd.119.087940
This article has not been copyedited and formatted. The final version may differ from this version.

Microsomal incubation. Preliminary assessments of microsomal protein concentration and incubation time to ensure linear metabolite formation over time were performed in pooled HLM (obtained commercially) for all probe substrates. Pooled HLM were also utilized for initial experiments evaluating repeatability in determination of V_{max} and K_m (coefficients of variation <15%). Activity incubations were carried out in 96-well plates at 37 °C and 300 rpm with hepatic and intestinal microsomal protein concentrations of 0.1-1 mg/mL (depending on available tissue amount) in 1 mmol/L phosphate buffer (pH 7.4) with 1 mmol/L NADPH. The microsome mixtures were preheated at 37 °C for 15 minutes and reactions initiated by adding probe substrate cocktail 1 or 2 at eight different concentrations (Table 1). Blank samples containing buffer, NADPH and substrates were also included. Methanol, in concentrations ≤1 %, was used in the incubations to keep substrates in solution. At 20 minutes, the incubation was stopped by transferring 20 µL of the incubation mixture to 60 µL of ice-cold ACN containing internal standard. The samples were centrifuged at 3,220 g for 20 minutes (4 °C), and the supernatant was transferred to a new plate and mixed with an equal volume of Milli-Q water. For samples with high analyte concentration, the 1:1 dilution was further diluted 1:20 with 30 % ACN.

Liquid chromatography tandem mass spectrometry. Quantification of probe metabolites was performed using a triple quadrupole mass spectrometer coupled to an ACQUITY UPLC® I-class system (Waters XevoTM TQ-S, Waters Corporation, Milford, MA, USA) equipped with an electrospray ionization source. The mass spectrometer was operated in multiple reaction monitoring mode. Samples were ionized in positive mode and the ion source was set to a temperature of 150 °C. Ionization source parameters were as follows: capillary voltage 0.60 kV, cone 60 V, source offset 60 V. Gas settings were as follows: cone gas 150 L/h, desolvation gas 1200 L/h and nebulizer gas flow 7 bar. Dwell time per transition was set to 0.010 seconds and mass transitions were determined by QuanOptimize (Waters Corporation, Milford, MA, USA) (Supplemental Table 1).

Chromatography was performed on an ACQUITY UPLC® HSS T3 column (2.1 × 50 mm, 1.8 µm particle size) at 40 °C. The flow rate was 0.8 mL/min and the injection volume was 5 µL. The mobile phases consisted of A: water, 0.2 % (v/v) formic acid and 2 % (v/v) ACN and B: ACN, 0.2 % (v/v) formic acid. The linear gradient was as follows: 0.2 % B from 0.00 to 0.30 min, 0.2 % to 95 % B from 0.30 to 1.60 min, 95 % B from 1.60 to 2.10 min, 95 % to 0.2 % B from 2.10 to 2.11 min, and 0.2 % B from 2.11 to 2.50 min. The run time was 2.50 min and the equilibration time between injections was 0.39 min.

Data was processed using TargetLynx^{TM} software (Waters Corporation, Milford, MA, USA). Concentrations were determined against matrix-spiked calibration standards over a range of 0.005-20 µmol/L. The calibration samples contained all seven metabolites (Table 1) and were analysed in triplicates. The calibration curves were fitted by weighted ($1/x^2$) linear least-square regression. Back-calculated values of calibrators within 80-120 % of nominal values (70-130 % for the lower limit of quantification) were accepted, and the residuals were inspected for homoscedasticity.

CYP genotyping. Analysis of CYP1A2, CYP2C9, CYP2C19, CYP2D6, CYP3A4 and CYP3A5 variant alleles were performed using Taqman-based real-time polymerase chain reaction assays implemented for routine pharmacogenetic analyses at the Center for Psychopharmacology, Diakonhjemmet Hospital. The following variant alleles were included in this study: CYP1A2: the increased induction allele *1F (rs762551); CYP2C9: the reduced-function alleles *2 (rs1799853) and *3 (rs1057910); CYP2C19: the null alleles *2 (rs4244285), *3 (rs4986893) and *4 (rs28399504) and the gain-of-function allele *17 (rs12248560); CYP2D6: the null alleles *3 (rs35742686), *4 (rs3892097), *5 (whole gene deletion) and *6 (rs5030655), the reduced-function alleles *9 (rs5030656), *10 (rs1065852) and *41 (rs28371725), as well as the increased-

DMD Fast Forward. Published on November 4, 2019 as DOI: 10.1124/dmd.119.087940
This article has not been copyedited and formatted. The final version may differ from this version.

function allele (whole gene duplication); CYP3A4: the reduced-function allele *22 (rs35599367); CYP3A5: the null allele *3 (rs776746).

Data analysis. Enzyme kinetic parameters were determined using untransformed data and GraphPad Prism 7® by fitting the reaction velocity versus substrate concentration data to the Michaelis-Menten model (equation 1) or the substrate inhibition model (equation 2):

Eq. 1 $$v = \frac{V_{max} \times S}{K_m + S}$$

Eq.2 $$v = \frac{V_{max} \times S}{K_m + S(1 + \frac{S}{K_i})}$$

where v is the velocity of the reaction, S is the substrate concentration, V_{max} is the maximum velocity, K_m is the Michaelis constant and K_i is the inhibitor constant.

As the incubations were performed with varying concentrations of microsomal protein, K_m values were adjusted for fraction of unbound drug (fu_{mic}). The fu_{mic} values were predicted from physicochemical properties of the substrates and microsomal protein concentration using the Simcyp prediction tool (Simcyp, 2016). Unbound intrinsic clearance ($CL_{int,u}$) was calculated from the ratio of V_{max} to $K_{m,u}$. Correlation coefficients were determined by Spearman rank order correlation analysis and significance levels of differences between groups were determined by Mann-Whitney U test using GraphPad Prism 7 (Graphpad software, USA).

DMD Fast Forward. Published on November 4, 2019 as DOI: 10.1124/dmd.119.087940
This article has not been copyedited and formatted. The final version may differ from this version.

Results

CYP activities in hepatic and small intestinal microsomes

Patient characteristics and diplotype/likely phenotype distribution for CYP1A2, CYP2C9, CYP2C19, CYP2D6, CYP3A4 and CYP3A5 are given in Table 2 and Table 3, respectively.

Activities of CYP2C8, CYP2C9, CYP2D6 and CYP3A were quantified in both human liver microsomes (HLM) and human intestinal microsomes (HIM), while activities of CYP1A2, CYP2B6 and CYP2C19 were only quantifiable in HLM. Enzyme kinetic parameters are summarized in Table 4 and Table 5 and representative enzyme kinetic curves are shown in Figure 1 and Figure 2. Substrate concentration versus velocity curves showed Michaelis-Menten enzyme kinetics, except for the formation of 1-OH-midazolam where the substrate inhibition model was used. Due to small liver tissue amounts and/or low enzyme activity, 4-OH-mephenytoin formation (CYP2C19) was only quantifiable in 13 of 20 individual HLM.

The $CL_{int,u}$ values were overall higher in the liver compared with the small intestine, with median HLM/HIM ratios of 5 (CYP2D6), 16 (CYP2C9) and 252 (CYP2C8) (Table 6). However, the CYP3A activities in HLM and HIM were comparable, with a median $CL_{int,u}$ HLM/HIM ratio of 1.5 (Table 6). While the median ratio of $K_{m,u}$ values in HLM and HIM was between 0.5 and 1.4 for all CYP enzymes investigated, the V_{max} values showed a larger interorgan difference with median HLM/HIM ratios ranging from 2 (CYP3A) to 196 (CYP2C8) (Table 6).

Both V_{max} and $K_{m,u}$ values showed large variability between patients, resulting in considerable interindividual variability in $CL_{int,u}$ values ranging from 9-fold (CYP3A) to 23-fold (CYP2B6) in HLM and from 5-fold (CYP2D6) to 55-fold (CYP2C9) in HIM (Table 4 and Table 5).

Hepatic $CL_{int,u}$ values for the CYP1A2 mediated reaction were significantly higher in patients with the **1/*1F* diplotype compared with the **1F/*1F* diplotype ($p<0.05$, Figure 3). This was

DMD Fast Forward. Published on November 4, 2019 as DOI: 10.1124/dmd.119.087940
This article has not been copyedited and formatted. The final version may differ from this version.

accompanied by significantly lower $K_{m,u}$ values in the **1/*1F* group ($p<0.05$), while no difference in V_{max} values was detected ($p>0.05$) (Supplemental Figure 1). Unbound intrinsic clearance values for the reactions mediated by CYP2C9, CYP2C19 or CYP2D6 were not significantly affected by diplotype or likely phenotype in HLM or HIM (Figure 3). The impact of *CYP3A5* diplotype on unbound intrinsic clearance for the CYP3A mediated reaction could not be investigated, since the *CYP3A5*1* allele was present in only one patient.

Interorgan correlation of CYP activities

A positive correlation ($r=0.74$, $p<0.001$) was found between the intestinal and hepatic microsomal $CL_{int,u}$ values for the formation of 4-OH-diclofenac (CYP2C9) (Figure 4). There were no significant correlations between $CL_{int,u}$ values in HLM and HIM for the probe reactions of CYP2C8, CYP2D6 or CYP3A (Figure 4).

Intraorgan correlation of CYP activities

Positive correlations were found between $CL_{int,u}$ values of reactions mediated by several different CYP isoforms in the HLM. The activity of CYP1A2 correlated positively with CYP2B6 ($r=0.51$), CYP2D6 ($r=0.58$) and CYP3A ($r=0.68$) activities (Table 7). Also, hepatic CYP2B6 activity was positively correlated with CYP2D6 ($r=0.60$) and CYP3A ($r=0.67$) activities (Table 7). There was a positive correlation between CYP2D6 and CYP3A activities in both HLM ($r=0.47$, Table 7) and HIM ($r=0.65$, Table 8). Furthermore, in HIM, the activity of CYP2C8 correlated positively with CYP2C9 ($r=0.53$), CYP2D6 ($r=0.50$) and CYP3A ($r=0.64$) activities (Table 8).

Correlation between BMI and CYP activities

There was a negative correlation between patient BMI and hepatic $CL_{int,u}$ values for the CYP2B6-mediated formation of OH-bupropion ($r=-0.72$, $p<0.001$, Figure 5). No significant

correlations were observed between BMI and the other hepatic CYP activities or between BMI and the intestinal CYP activities (data not shown).

Sex differences in CYP activities

The small intestinal $CL_{int,u}$ values for the CYP3A mediated reaction were significantly higher in the female individuals (median of 33 µL/min/mg protein) compared with the male individuals (median of 18 µL/min/mg protein) ($p<0.05$, Figure 6). No difference in hepatic CYP3A activity between sexes was detected ($p>0.05$, Figure 6). No differences between sexes were observed for hepatic or intestinal activities of the other CYP enzymes (data not shown).

Discussion

Data on hepatic and intestinal CYP metabolism is relevant with respect to evaluation of susceptibility to drug-drug interactions, assessment of oral bioavailability in drug development and prediction of drug disposition in different patient populations. To our knowledge, this is the first study to investigate the activities of drug metabolizing CYP enzymes in microsomes prepared from paired liver and small intestinal biopsies from patients with obesity.

Considerable interindividual variability in both hepatic (up to 23-fold) and intestinal (up to 55-fold) unbound intrinsic clearance values of CYP probe reactions was observed in the present study. While CYP activities have been mostly investigated in pooled microsomal preparations, large variability in enzyme kinetic parameters has also been reported in a limited number of studies in individual HLM and HIM from other patient populations (Clermont et al., 2019; Gao et al., 2016; Madani et al., 1999; Obach et al., 2001; Paine et al., 1997; Yang et al., 2012). Hepatic intrinsic clearance values of the investigated CYP probes in this study were mostly in the lower end of the range of those reported in another study in Caucasians (Yang et al., 2012). Similarly, intestinal intrinsic clearance values for the CYP3A mediated reaction were within or slightly lower than the ranges previously reported in individual jejunal microsomes (Clermont et al., 2019; Paine et al., 1997). To what extent these moderately lower activities are related to the specific patient population investigated is difficult to evaluate, as some variation across studies may also be due to methodological factors. Furthermore, an overall lower interindividual variability in CYP activities in both tissues was found in the current study, which could possibly be explained by this study being performed in a more homogenous patient group. Interestingly, the *CYP1A2* diplotype significantly affected the activity of CYP1A2 in HLM, while activities of the other CYP enzymes were not affected by diplotype or likely phenotype. However, the number of samples analysed may be too low to disclose differences between genotypes.

DMD Fast Forward. Published on November 4, 2019 as DOI: 10.1124/dmd.119.087940
This article has not been copyedited and formatted. The final version may differ from this version.

As expected, the microsomal CYP activities were overall considerably higher in the liver compared with the small intestine. However, the ratios showed large variability, suggesting that the contribution of the small intestine to the first pass metabolism of CYP2D6 and CYP2C9 substrates could vary considerably between individuals. For CYP2C8, the intestinal activities were negligible compared with the hepatic activities, in line with a previous study comparing pooled HLM and HIM (Misaka et al., 2013). On the contrary, microsomal CYP3A activities were comparable with a 1.5-fold higher median $CL_{int,u}$ value in HLM compared with the HIM. This is in agreement with the ratio between hepatic and jejunal microsomal CYP3A activities reported in paired samples by Paine et al. (1997), as well as with recent studies in subjects both with and without obesity finding comparable mRNA and protein content of CYP3A4 in paired liver and jejunum samples (Drozdzik et al., 2017; Lloret-Linares et al., 2019). This underlines the likely important role of the small intestine in the first pass metabolism of CYP3A substrates also in this patient population.

A positive correlation between CYP2C9 activities in HLM and HIM was found. This is in line with a study reporting a borderline significant positive correlation between CL_{int} values for the 4-hydroxylation of diclofenac in hepatic and intestinal homogenates (Läpple et al., 2003), as well as with a recent study in patients with obesity showing a positive correlation between expression levels of CYP2C9 in hepatic and jejunal microsomes (Lloret-Linares et al., 2019). It could be speculated that this is partly explained by the activity of CYP2C9 being largely influenced by genetics (Zanger and Schwab, 2013), but interestingly, however, no correlation was found between hepatic and intestinal activities of the highly polymorphic enzyme CYP2D6. Also, no interorgan correlation was present for the activities of CYP2C8 and CYP3A, which is in agreement with other studies (Lin et al., 2002; Lown et al., 1994; Läpple et al., 2003; Paine et al., 1997; von Richter et al., 2004). The lack of interorgan associations may be related to tissue-specific regulation due to both differential expression patterns of CYP regulating transcription

DMD Fast Forward. Published on November 4, 2019 as DOI: 10.1124/dmd.119.087940
This article has not been copyedited and formatted. The final version may differ from this version.

factors in the small intestine and liver, as well as exposure to different endogenous and environmental factors (Pavek and Dvorak, 2008). For CYP3A4, the vitamin D receptor has been shown to be an important nuclear receptor involved in inducible transcriptional regulation of CYP3A4 in the intestine, but not in the liver (Khan et al., 2010; Matsubara et al., 2008; Thirumaran et al., 2012). Furthermore, positive correlations between activities of different CYP isoforms were found in both HLM and HIM in the present study. This is in line with other studies of expression and activities of CYP enzymes in human liver samples (Gao et al., 2016; Wortham et al., 2007; Yang et al., 2012; Yang et al., 2010), while limited data currently exists on the association between CYP isoforms in the human intestine (Lindell et al., 2003; Obach et al., 2001). Intraorgan correlations of CYP activities may in part be explained by shared regulatory pathways within the liver and intestine, as the expression of some CYP isoforms is regulated by common transcription factors (Manikandan and Nagini, 2018; Wortham et al., 2007). Also, post-transcriptional co-regulation of enzyme activities may occur via NADPH-cytochrome P450 oxidoreductase and cytochrome b_5 (Wortham et al., 2007; Zhang et al., 2015; Zhang et al., 2016).

Interestingly, the present study showed significantly higher $CL_{int,u}$ for the 1-hydroxylation of midazolam in individual HIM from females compared with males. In agreement with this, increased oral clearance of CYP3A substrates and higher small intestinal CYP3A activity have been reported in females compared with males (Chen et al., 2006; Kang et al., 2003; Lampen et al., 1996; Lown et al., 1994). However, a recent study of CYP expression in jejunum from patients with severe obesity found no sex differences (Miyauchi et al., 2016). Findings in human liver samples have been conflicting (George et al., 1995; Hunt et al., 1992; Shimada et al., 1994; Wolbold et al., 2003), and in the current study, no difference in hepatic CYP3A activities between sexes was detected. Our observations could suggest higher CYP3A activity in the small intestine, but not in the liver, of female compared with male individuals with obesity. However,

given the low sample size, and especially the low number of male subjects, this needs to be validated in a larger study.

In the present study, we found a negative correlation between BMI and hepatic CYP2B6 activity in patients with obesity, which has to the authors' knowledge not been previously reported. It is difficult to comment on possible mechanisms behind this finding. In general, it could be speculated that reductions in CYP activity with increasing weight is related to inflammation status, as inflammatory cytokines have been found to alter the expression and activity of various CYP enzymes in hepatocytes and/or HepaRG cells (Aitken and Morgan, 2007; Rubin et al., 2015). However, no correlation between BMI and activity was found for the other CYP enzymes investigated. Furthermore, it must be emphasized that the validity of this finding is challenged by the low sample size. Further studies in individuals ranging from normal weight to severe obesity is required to elucidate the effect of obesity on drug metabolizing CYP enzymes in the liver.

This study has some limitations. While microsomes are the most commonly used matrix for studying drug metabolism *in vitro*, this approach has some drawbacks. The preparation of microsomes through subcellular fractionation has been associated with both loss of microsomal protein and contamination of the microsomal fraction with non-microsomal proteins (Wegler et al., 2017). We did not account for this through the use of a microsomal protein marker. Also, the intestinal samples were homogenized directly without prior mucosal scraping or enterocyte elution. Thus, microsomal fractions were prepared from homogenate containing not only the mature enterocytes where the CYP enzymes are concentrated (Galetin and Houston, 2006; Hatley et al., 2017). Furthermore, an important challenge associated with studying human biopsies is that the observations in a small tissue sample may not be representative for the whole organ, thereby complicating *in vitro-in vivo* extrapolation. This is particularly relevant for the intestinal biopsies, given the heterogeneity of the gastrointestinal tract. It should therefore be

emphasized that CYP activities in the present study is estimated per milligram of microsomal protein and scaling up to whole organ activities is necessary in order to fully compare the CYP metabolism in these two tissues. It should also be noted that the patients were subjected to a three-week low energy diet prior to biopsy harvesting, which has been shown to significantly reduce liver volume and intrahepatic fat (Edholm et al., 2011). The data presented may therefore not be fully transferrable to patients with untreated severe obesity. Finally, it must be emphasized that no a priori power calculation was performed and that the study population was relatively small.

In conclusion, data on CYP activities in paired liver and small intestinal samples presented in the current study may be useful for modelling and prediction of drug disposition in patients with obesity.

Acknowledgements

We express our gratitude to the participants, the surgical staff and to the study personnel in the COCKTAIL study.

Authorship contributions

Participated in research design: Krogstad, Peric, Robertsen, Kringen, Wegler, Hjelmesæth, Karlsson, S. Andersson, Artursson, Åsberg, T.B. Andersson, and Christensen.

Conducted experiments: Krogstad, Peric, Kringen, and Angeles.

Contributed new reagents or analytic tools: Peric, and T.B. Andersson.

Performed data analysis: Krogstad, Peric, Robertsen, T.B. Andersson, and Christensen.

Wrote or contributed to the writing of the manuscript: Krogstad, Peric, Robertsen, Kringen, Wegler, Angeles, Hjelmesæth, Karlsson, S. Andersson, Artursson, Åsberg, T.B. Andersson, and Christensen.

References

Achour B, Barber J, and Rostami-Hodjegan A (2014) Expression of hepatic drug-metabolizing cytochrome P450 enzymes and their intercorrelations: a meta-analysis. *Drug Metab Dispos* **42**: 1349-1356.

Aitken AE, and Morgan ET (2007) Gene-specific effects of inflammatory cytokines on cytochrome P450 2C, 2B6 and 3A4 mRNA levels in human hepatocytes. *Drug Metab Dispos* **35**: 1687-1693.

Birdwell KA, Decker B, Barbarino JM, Peterson JF, Stein CM, Sadee W, Wang D, Vinks AA, He Y, Swen JJ, Leeder JS, van Schaik R, Thummel KE, Klein TE, Caudle KE, and MacPhee IA (2015) Clinical Pharmacogenetics Implementation Consortium (CPIC) guidelines for CYP3A5 genotype and tacrolimus dosing. *Clin Pharmacol Ther* **98**: 19-24.

Bradford MM (1976) A rapid and sensitive method for the quantitation of microgram quantities of protein utilizing the principle of protein-dye binding. *Anal Biochem* **72**: 248-254.

Brill MJ, Diepstraten J, van Rongen A, van Kralingen S, van den Anker JN, and Knibbe CA (2012) Impact of obesity on drug metabolism and elimination in adults and children. *Clin Pharmacokinet* **51**: 277-304.

Brown JT, Bishop JR, Sangkuhl K, Nurmi EL, Mueller DJ, Dinh JC, Gaedigk A, Klein TE, Caudle KE, McCracken JT, de Leon J, and Leeder JS (2019) Clinical Pharmacogenetics Implementation Consortium (CPIC) guideline for CYP2D6 genotype and atomoxetine therapy. *Clin Pharmacol Ther* **106**: 94-102.

Caudle KE, Rettie AE, Whirl-Carrillo M, Smith LH, Mintzer S, Lee MT, Klein TE, and Callaghan JT (2014) Clinical Pharmacogenetics Implementation Consortium guidelines for CYP2C9 and HLA-B genotypes and phenytoin dosing. *Clin Pharmacol Ther* **96**: 542-548.

Chen M, Ma L, Drusano GL, Bertino JS, Jr., and Nafziger AN (2006) Sex differences in CYP3A activity using intravenous and oral midazolam. *Clin Pharmacol Ther* **80**: 531-538.

Clermont V, Grangeon A, Barama A, Turgeon J, Lallier M, Malaise J, and Michaud V (2019) Activity and mRNA expression levels of selected cytochromes P450 in various sections of the human small intestine. *Br J Clin Pharmacol* **85**: 1367-1377.

Drozdzik M, Busch D, Lapczuk J, Muller J, Ostrowski M, Kurzawski M, and Oswald S (2017) Protein abundance of clinically relevant drug-metabolizing enzymes in the human liver and intestine: a comparative analysis in paired tissue specimens. *Clin Pharmacol Ther* **104**: 515-524.

Edholm D, Kullberg J, Haenni A, Karlsson FA, Ahlstrom A, Hedberg J, Ahlstrom H, and Sundbom M (2011) Preoperative 4-week low-calorie diet reduces liver volume and intrahepatic fat, and facilitates laparoscopic gastric bypass in morbidly obese. *Obes Surg* **21**: 345-350.

Galetin A, and Houston JB (2006) Intestinal and hepatic metabolic activity of five cytochrome P450 enzymes: impact on prediction of first-pass metabolism. *J Pharmacol Exp Ther* **318**: 1220-1229.

Gao N, Tian X, Fang Y, Zhou J, Zhang H, Wen Q, Jia L, Gao J, Sun B, Wei J, Zhang Y, Cui M, and Qiao H (2016) Gene polymorphisms and contents of cytochrome P450s have only limited effects on metabolic activities in human liver microsomes. *Eur J Pharm Sci* **92**: 86-97.

George J, Byth K, and Farrell GC (1995) Age but not gender selectively affects expression of individual cytochrome P450 proteins in human liver. *Biochem Pharmacol* **50**: 727-730.

Hatley OJ, Jones CR, Galetin A, and Rostami-Hodjegan A (2017) Quantifying gut wall metabolism: methodology matters. *Biopharm Drug Dispos* **38**: 155-160.

Hjelmesæth J, Asberg A, Andersson S, Sandbu R, Robertsen I, Johnson LK, Angeles PC, Hertel JK, Skovlund E, Heijer M, Ek AL, Krogstad V, Karlsen TI, Christensen H, Andersson TB, and Karlsson C (2018) Impact of body weight, low energy diet and gastric bypass on drug bioavailability, cardiovascular risk factors and metabolic biomarkers: protocol for an

open, non-randomised, three-armed single centre study (COCKTAIL). *BMJ Open* **8**: e021878.

Hunt CM, Westerkam WR, and Stave GM (1992) Effect of age and gender on the activity of human hepatic CYP3A. *Biochem Pharmacol* **44**: 275-283.

Ingelman-Sundberg M (2005) The human genome project and novel aspects of cytochrome P450 research. *Toxicol Appl Pharmacol* **207**: 52-56.

Kang D, Verotta D, Krecic-Shepard ME, Modi NB, Gupta SK, and Schwartz JB (2003) Population analyses of sustained-release verapamil in patients: effects of sex, race, and smoking. *Clin Pharmacol Ther* **73**: 31-40.

Khan AA, Dragt BS, Porte RJ, and Groothuis GM (2010) Regulation of VDR expression in rat and human intestine and liver-consequences for CYP3A expression. *Toxicol In Vitro* **24**: 822-829.

Lampen A, Christians U, Bader A, Hackbarth I, and Sewing KF (1996) Drug interactions and interindividual variability of ciclosporin metabolism in the small intestine. *Pharmacology* **52**: 159-168.

Lin YS, Dowling AL, Quigley SD, Farin FM, Zhang J, Lamba J, Schuetz EG, and Thummel KE (2002) Co-regulation of CYP3A4 and CYP3A5 and contribution to hepatic and intestinal midazolam metabolism. *Mol Pharmacol* **62**: 162-172.

Lindell M, Karlsson MO, Lennernas H, Pahlman L, and Lang MA (2003) Variable expression of CYP and Pgp genes in the human small intestine. *Eur J Clin Invest* **33**: 493-499.

Lloret-Linares C, Daali Y, Abbara C, Carette C, Bouillot JL, Vicaut E, Czernichow S, and Decleves X (2019) CYP450 activities before and after Roux-en-Y gastric bypass: correlation with their intestinal and liver content. *Surg Obes Relat Dis* **15**: 1299-1310.

Lown KS, Kolars JC, Thummel KE, Barnett JL, Kunze KL, Wrighton SA, and Watkins PB (1994) Interpatient heterogeneity in expression of CYP3A4 and CYP3A5 in small bowel. Lack of prediction by the erythromycin breath test. *Drug Metab Dispos* **22**: 947-955.

Läpple F, von Richter O, Fromm MF, Richter T, Thon KP, Wisser H, Griese EU, Eichelbaum M, and Kivisto KT (2003) Differential expression and function of CYP2C isoforms in human intestine and liver. *Pharmacogenetics* **13**: 565-575.

Madani S, Paine MF, Lewis L, Thummel KE, and Shen DD (1999) Comparison of CYP2D6 content and metoprolol oxidation between microsomes isolated from human livers and small intestines. *Pharm Res* **16**: 1199-1205.

Manikandan P, and Nagini S (2018) Cytochrome P450 structure, function and clinical significance: a review. *Curr Drug Targets* **19**: 38-54.

Matsubara T, Yoshinari K, Aoyama K, Sugawara M, Sekiya Y, Nagata K, and Yamazoe Y (2008) Role of vitamin D receptor in the lithocholic acid-mediated CYP3A induction in vitro and in vivo. *Drug Metab Dispos* **36**: 2058-2063.

Misaka S, Kawabe K, Onoue S, Werba JP, Giroli M, Tamaki S, Kan T, Kimura J, Watanabe H, and Yamada S (2013) Effects of green tea catechins on cytochrome P450 2B6, 2C8, 2C19, 2D6 and 3A activities in human liver and intestinal microsomes. *Drug Metab Pharmacokinet* **28**: 244-249.

Miyauchi E, Tachikawa M, Decleves X, Uchida Y, Bouillot JL, Poitou C, Oppert JM, Mouly S, Bergmann JF, Terasaki T, Scherrmann JM, and Lloret-Linares C (2016) Quantitative atlas of cytochrome P450, UDP-glucuronosyltransferase, and transporter proteins in jejunum of morbidly obese subjects. *Mol Pharm* **13**: 2631-2640.

Morgan ET, Goralski KB, Piquette-Miller M, Renton KW, Robertson GR, Chaluvadi MR, Charles KA, Clarke SJ, Kacevska M, Liddle C, Richardson TA, Sharma R, and Sinal CJ (2008) Regulation of drug-metabolizing enzymes and transporters in infection, inflammation, and cancer. *Drug Metab Dispos* **36**: 205-216.

Moriyama B, Obeng AO, Barbarino J, Penzak SR, Henning SA, Scott SA, Agundez J, Wingard JR, McLeod HL, Klein TE, Cross SJ, Caudle KE, and Walsh TJ (2017) Clinical

Pharmacogenetics Implementation Consortium (CPIC) guidelines for CYP2C19 and voriconazole therapy. *Clin Pharmacol Ther* **102**: 45-51.

Obach RS, Zhang QY, Dunbar D, and Kaminsky LS (2001) Metabolic characterization of the major human small intestinal cytochrome P450s. *Drug Metab Dispos* **29**: 347-352.

Paine MF, Hart HL, Ludington SS, Haining RL, Rettie AE, and Zeldin DC (2006) The human intestinal cytochrome P450 "pie". *Drug Metab Dispos* **34**: 880-886.

Paine MF, Khalighi M, Fisher JM, Shen DD, Kunze KL, Marsh CL, Perkins JD, and Thummel KE (1997) Characterization of interintestinal and intraintestinal variations in human CYP3A-dependent metabolism. *J Pharmacol Exp Ther* **283**: 1552-1562.

Pavek P, and Dvorak Z (2008) Xenobiotic-induced transcriptional regulation of xenobiotic metabolizing enzymes of the cytochrome P450 superfamily in human extrahepatic tissues. *Curr Drug Metab* **9**: 129-143.

Rubin K, Janefeldt A, Andersson L, Berke Z, Grime K, and Andersson TB (2015) HepaRG cells as human-relevant in vitro model to study the effects of inflammatory stimuli on cytochrome P450 isoenzymes. *Drug Metab Dispos* **43**: 119-125.

Shah RR, and Smith RL (2015) Inflammation-induced phenoconversion of polymorphic drug metabolizing enzymes: hypothesis with implications for personalized medicine. *Drug Metab Dispos* **43**: 400-410.

Shimada T, Yamazaki H, Mimura M, Inui Y, and Guengerich FP (1994) Interindividual variations in human liver cytochrome P-450 enzymes involved in the oxidation of drugs, carcinogens and toxic chemicals: studies with liver microsomes of 30 Japanese and 30 Caucasians. *J Pharmacol Exp Ther* **270**: 414-423.

Simcyp (2016) Simcyp prediction tools-fumic. Retrieved from https://members.simcyp.com/account/tools/fumic

Spaggiari D, Geiser L, Daali Y, and Rudaz S (2014) A cocktail approach for assessing the in vitro activity of human cytochrome P450s: an overview of current methodologies. *J Pharm Biomed Anal* **101**: 221-237.

Thirumaran RK, Lamba JK, Kim RB, Urquhart BL, Gregor JC, Chande N, Fan Y, Qi A, Cheng C, Thummel KE, Hall SD, and Schuetz EG (2012) Intestinal CYP3A4 and midazolam disposition in vivo associate with VDR polymorphisms and show seasonal variation. *Biochem Pharmacol* **84**: 104-112.

Thorn CF, Aklillu E, Klein TE, and Altman RB (2012) PharmGKB summary: very important pharmacogene information for CYP1A2. *Pharmacogenet Genomics* **22**: 73-77.

Tian DD, Natesan S, White Jr, Jr., and Paine MF (2019) Effects of common CYP1A2 genotypes and other key factors on intraindividual variation in the caffeine metabolic ratio: an exploratory analysis. *Clin Transl Sci* **12**: 39-46.

Ulvestad M, Skottheim IB, Jakobsen GS, Bremer S, Molden E, Asberg A, Hjelmesaeth J, Andersson TB, Sandbu R, and Christensen H (2013) Impact of OATP1B1, MDR1, and CYP3A4 expression in liver and intestine on interpatient pharmacokinetic variability of atorvastatin in obese subjects. *Clin Pharmacol Ther* **93**: 275-282.

von Richter O, Burk O, Fromm MF, Thon KP, Eichelbaum M, and Kivisto KT (2004) Cytochrome P450 3A4 and P-glycoprotein expression in human small intestinal enterocytes and hepatocytes: a comparative analysis in paired tissue specimens. *Clin Pharmacol Ther* **75**: 172-183.

Wegler C, Gaugaz FZ, Andersson TB, Wisniewski JR, Busch D, Groer C, Oswald S, Noren A, Weiss F, Hammer HS, Joos TO, Poetz O, Achour B, Rostami-Hodjegan A, van de Steeg E, Wortelboer HM, and Artursson P (2017) Variability in mass spectrometry-based quantification of clinically relevant drug transporters and drug metabolizing enzymes. *Mol Pharm* **14**: 3142-3151.

Wolbold R, Klein K, Burk O, Nussler AK, Neuhaus P, Eichelbaum M, Schwab M, and Zanger UM (2003) Sex is a major determinant of CYP3A4 expression in human liver. *Hepatology* **38**: 978-988.

Wortham M, Czerwinski M, He L, Parkinson A, and Wan YJ (2007) Expression of constitutive androstane receptor, hepatic nuclear factor 4 alpha, and P450 oxidoreductase genes determines interindividual variability in basal expression and activity of a broad scope of xenobiotic metabolism genes in the human liver. *Drug Metab Dispos* **35**: 1700-1710.

Yang J, He MM, Niu W, Wrighton SA, Li L, Liu Y, and Li C (2012) Metabolic capabilities of cytochrome P450 enzymes in Chinese liver microsomes compared with those in Caucasian liver microsomes. *Br J Clin Pharmacol* **73**: 268-284.

Yang X, Zhang B, Molony C, Chudin E, Hao K, Zhu J, Gaedigk A, Suver C, Zhong H, Leeder JS, Guengerich FP, Strom SC, Schuetz E, Rushmore TH, Ulrich RG, Slatter JG, Schadt EE, Kasarskis A, and Lum PY (2010) Systematic genetic and genomic analysis of cytochrome P450 enzyme activities in human liver. *Genome Res* **20**: 1020-1036.

Zanger UM, and Schwab M (2013) Cytochrome P450 enzymes in drug metabolism: regulation of gene expression, enzyme activities, and impact of genetic variation. *Pharmacol Ther* **138**: 103-141.

Zhang HF, Gao N, Liu TT, Fang Y, Qi B, Wen Q, Zhou J, Jia LJ, and Qiao HL (2015) Effect of cytochrome b5 content on the activity of polymorphic CYP1A2, 2B6, and 2E1 in human liver microsomes. *PLoS One* **10**: e0128547.

Zhang HF, Li ZH, Liu JY, Liu TT, Wang P, Fang Y, Zhou J, Cui MZ, Gao N, Tian X, Gao J, Wen Q, Jia LJ, and Qiao HL (2016) Correlation of cytochrome P450 oxidoreductase expression with the expression of 10 isoforms of cytochrome P450 in human liver. *Drug Metab Dispos* **44**: 1193-1200.

Figure legends

Figure 1. Representative reaction velocity versus substrate concentration curves for the formation of metabolites used as probe reactions for the activities of CYP1A2, CYP2B6, CYP2C8, CYP2C9, CYP2C19, CYP2D6, and CYP3A in human liver microsomes (HLM). Details of the CYP activity assays are described under *Microsomal incubation*. *Data points of the two highest substrate concentrations were excluded due to sharp drops in the curves for which the reason is unknown.

Figure 2. Representative reaction velocity versus substrate concentration curves for the formation of metabolites used as probe reactions for the activities of CYP2C8, CYP2C9, CYP2D6 and CYP3A in human intestinal microsomes (HIM). Details of the CYP activity assays are described under *Microsomal incubation*.

Figure 3. Unbound intrinsic clearance ($CL_{int,u}$) values for the reactions mediated by CYP1A2, CYP2C9, CYP2C19 and CYP2D6 in human liver microsomes (HLM) and by CYP2C9 and CYP2D6 in human intestinal microsomes (HIM) grouped by the respective CYP diplotype or likely phenotype. The lines represent the median in each group.*Difference between groups was statistically significant ($p<0.05$). NM, normal metabolizer; IM, intermediate metabolizer; PM, poor metabolizer; RM, rapid metabolizer; UM, ultrarapid metabolizer

Figure 4. Correlation between unbound intrinsic clearance ($CL_{int,u}$) in human liver microsomes (HLM) and human intestinal microsomes (HIM) for amodiaquine N-deethylation (CYP2C8), diclofenac 4-hydroxylation (CYP2C9), bufuralol 1-hydroxylation (CYP2D6) and midazolam 1-hydroxylation (CYP3A) in individual patients. Dotted linear trend line added for visualization purposes.

Figure 5. Correlation between body mass index (BMI) and unbound intrinsic clearance ($CL_{int,u}$) for the bupropion hydroxylation (CYP2B6) in human liver microsomes (HLM). For visualization

purposes, the y-axis has been logarithmically transformed and a dotted linear trend line has been added.

Figure 6. Unbound intrinsic clearance ($CL_{int,u}$) values for the 1-hydroxylation of midazolam (CYP3A, µL/min/mg protein) in human intestinal microsomes (HIM) and human hepatic microsomes (HLM) from females and males. The lines represent the median in each group. *Difference between males and females was statistically significant ($p<0.05$).

DMD Fast Forward. Published on November 4, 2019 as DOI: 10.1124/dmd.119.087940
This article has not been copyedited and formatted. The final version may differ from this version.

Table 1 Substrates, substrate concentrations and metabolites used as probe reactions for the respective CYP enzyme activities

	Enzyme	Substrate	Substrate concentration range (μM)	Metabolite
Cocktail 1	CYP2B6	Bupropion	1.6-200	OH-bupropion
	CYP2C8	Amodiaquine	0.4-50	N-Desethylamodiaquine
	CYP2C9	Diclofenac	0.8-100	4-OH-diclofenac
	CYP2D6	Bufuralol	0.8-100	1-OH-bufuralol
	CYP3A	Midazolam	0.8-100	1-OH-midazolam
Cocktail 2	CYP1A2	Phenacetin	1.6-200	Paracetamol
	CYP2C19	S-Mephenytoin	0.8-100	4-OH-mephenytoin

DMD Fast Forward. Published on November 4, 2019 as DOI: 10.1124/dmd.119.087940
This article has not been copyedited and formatted. The final version may differ from this version.

Table 2 Patient characteristics, described as median and range or absolute numbers at the time of biopsy obtainment

Characteristic	Median and range or absolute numbers	
	Females (n=14)	*Males (n=6)*
Age (years)	46 (27-57)	49 (43-53)
Total body weight (kg)	118 (95-166)	143 (123-147)
Body mass index (kg/m^2)	43 (35-63)	45 (40-46)
Waist circumference (cm)	119 (97-142)	134 (128-140)
Hip circumference (cm)	131 (110-179)	127 (121-133)
Systolic blood pressure (mmHg)	120 (106-172)	116 (103-130)
Diastolic blood pressure (mmHg)	81 (71-106)	76 (65-81)
Total cholesterol (mmol/L)	3.7 (1.9-5.3)	3.3 (2.4-4.4)
HbA1c (mmol/mol)	38 (34-45)	38 (34-45)
eGFR (CKD-EPI; mL/min/1.73m^2)	109 (91-125)	110 (104-126)
ASAT (U/L)	25 (15-44)	32 (21-48)
ALAT (U/L)	31 (11-89)	51 (17-78)
ALP (U/L)	68 (27-102)	72 (56-110)
Albumin (g/L)	40 (16-44)	43 (38-44)
hs-CRP (mg/L)	3.0 (1.4-19.0)	5.5 (1.8-10.0)
Comorbidity		
Type 2 diabetes	3	0
Hypertension	5	4
Obstructive sleep apnea	7	6
Asthma	2	2
Cholelithiasis	4	0
Present smokers	0	0

HbA1c, glycated hemoglobin; eGFR, estimated glomerular filtration rate; ASAT, aspartate aminotransferase; ALAT, alanine aminotransferase; ALP, alkaline phosphatase; hs-CRP, high-sensitivity C-reactive protein

DMD Fast Forward. Published on November 4, 2019 as DOI: 10.1124/dmd.119.087940
This article has not been copyedited and formatted. The final version may differ from this version.

Table 3 Distribution of CYP1A2, CYP2C9, CYP2C19, CYP2D6, CYP3A4 and CYP3A5 diplotypes and likely phenotypes in patients included in the present study

Enzyme	Diplotype	Likely phenotype	n	
CYP1A2	**1/*1*	NM	1	(Thorn et al., 2012; Tian et al., 2019)
	**1/*1F*	Hyperinducer	9	
	**1F/*1F*	Hyperinducer	10	
CYP2C9	**1/*1*	NM	15	(Caudle et al., 2014)
	**1/*2*	IM	5	
CYP2C19	**17/*17*	UM	1	(Moriyama et al., 2017)
	**1/*17*	RM	8	
	**1/*1*	NM	5	
	**1/*2*	IM	4	
	**2/*17*	IM	1	
	**2/*2*	PM	1	
CYP2D6	**1/*1*	NM	8	(Brown et al., 2019)
	**1/*9*	NM	2	
	**1/*41*	NM	3	
	**1/*4*	IM	5	
	**4/*10*	IM	1	
	**5/*5*	PM	1	
CYP3A4	**1/*1*	NM	20	
CYP3A5	**1/*3*	IM	1	(Birdwell et al., 2015)
	**3/*3*	PM	19	

NM, normal metabolizer; IM, intermediate metabolizer; PM, poor metabolizer; RM, rapid metabolizer; UM, ultrarapid metabolizer

Table 4 Enzyme kinetic parameters (presented as median, range and max/min ratio) for metabolite formations representative of CYP1A2, CYP2B6, CYP2C8, CYP2C9, CYP2C19, CYP2D6 and CYP3A activities in human liver microsomes

Enzyme/metabolite	n	V_{max}				$K_{m,u}$				$CL_{int,u}$			
		Median	Max	Min	Max/Min	Median	Max	Min	Max/Min	Median	Max	Min	Max/Min
		nmol/min/mg protein				*µM*				*µL/min/mg protein*			
CYP1A2 Paracetamol	20	0.201	0.329	0.048	7	52	575	17	34	2.1	8.6	0.6	15
CYP2B6 OH-bupropion	20	0.067	0.445	0.016	28	47	189	20	9	1.4	11.9	0.5	23
CYP2C8 N-Desethylamodiaquine	20	0.523	0.963	0.123	8	4	13	1	12	108	604	31	19
CYP2C9 4-OH-diclofenac	20	1.054	1.865	0.392	5	25	68	10	7	39	140	6	22
CYP2C19 4-OH-mephenytoin	13	0.030	0.092	0.010	9	32	107	8	14	1.3	2.9	0.2	17
CYP2D6 1-OH-bufuralol	20	0.012	0.038	0.005	8	24	56	10	6	0.5	1.6	0.1	14
CYP3A 1-OH-midazolam	20	0.164	0.534	0.073	7	4	7	3	3	39	126	14	9

$K_{m,u}$, unbound Michaelis constant; V_{max}, maximum velocity; $CL_{int,u}$, unbound intrinsic clearance

Table 5 Enzyme kinetic parameters (presented as median, range and max/min ratio) for metabolite formation as representative of CYP2C8, CYP2C9, CYP2D6 and CYP3A activities in human intestinal microsomes

Enzyme/metabolite	n	V_{max}				$K_{m,u}$				$CL_{int,u}$			
		Median	Max	Min	Max/Min	Median	Max	Min	Max/Min	Median	Max	Min	Max/Min
		nmol/min/mg protein				*µM*				*µL/min/mg protein*			
CYP1A2 Paracetamol	20	No detectable activity											
CYP2B6 OH-bupropion	20	No detectable activity											
CYP2C8 N-Desethylamodiaquine	20	0.003	0.007	0.001	5	6	10	2	6	0.5	2.1	0.2	11
CYP2C9 4-OH-diclofenac	20	0.056	0.213	0.008	26	17	59	2	38	2.9	17.1	0.3	55
CYP2C19 4-OH-mephenytoin	20	No detectable activity											
CYP2D6 1-OH-bufuralol	20	0.004	0.009	0.003	3	48	70	33	2	0.09	0.20	0.04	5
CYP3A 1-OH-midazolam	20	0.090	0.237	0.034	7	3	6	2	2	31	59	8	7

$K_{m,u}$, unbound Michaelis constant; V_{max}, maximum velocity; $CL_{int,u}$, unbound intrinsic clearance

DMD Fast Forward. Published on November 4, 2019 as DOI: 10.1124/dmd.119.087940
This article has not been copyedited and formatted. The final version may differ from this version.

Table 6 Ratios of enzyme kinetic parameters for the probe reactions of CYP2C8, CYP2C9, CYP2D6 and CYP3A in individual human liver microsomes (HLM) and human intestinal microsomes (HIM) presented as median and range

Enzyme/metabolite	n	Ratio HLM/HIM		
		V_{max}	$K_{m,u}$	$CL_{int,u}$
CYP2C8 N-Desethylamodiaquine	20	196 (22-410)	0.8 (0.1-4.0)	252 (40-1544)
CYP2C9 4-OH-diclofenac	20	23 (5-67)	1.4 (0.9-14.5)	16 (4-26)
CYP2D6 1-OH-bufuralol	20	3.2 (1.0-6.0)	0.5 (0.2-1.6)	4.6 (1.7-22.8)
CYP3A 1-OH-midazolam	20	2.3 (0.4-4.9)	1.4 (0.7-2.2)	1.5 (0.4-4.4)

$K_{m,u}$, unbound Michaelis constant; V_{max}, maximum velocity; $CL_{int,u,}$ unbound intrinsic clearance

DMD Fast Forward. Published on November 4, 2019 as DOI: 10.1124/dmd.119.087940
This article has not been copyedited and formatted. The final version may differ from this version.

Table 7 Correlation coefficients (Spearman's rho) between unbound intrinsic clearance ($CL_{int,u}$) values of CYP isoforms in human liver microsomes

	CYP1A2	CYP2B6	CYP2C8	CYP2C9	CYP2C19	CYP2D6
CYP2B6	**0.51***					
CYP2C8	0.09	0.13				
CYP2C9	-0.22	-0.07	0.32			
CYP2C19	0.02	0.24	-0.55	0.02		
CYP2D6	**0.58****	**0.60****	0.25	-0.26	-0.30	
CYP3A	**0.68*****	**0.67****	0.36	-0.15	-0.36	**0.47***

*p < 0.05, **p < 0.01, ***p < 0.001

DMD Fast Forward. Published on November 4, 2019 as DOI: 10.1124/dmd.119.087940
This article has not been copyedited and formatted. The final version may differ from this version.

Table 8 Correlation coefficients (Spearman's rho) between unbound intrinsic clearance ($CL_{int,u}$) values of CYP isoforms in human intestinal microsomes

	CYP2C8	CYP2C9	CYP2D6
CYP2C9	**0.53***		
CYP2D6	**0.50***	0.00	
CYP3A	**0.64****	0.22	**0.65****

*p < 0.05, **p < 0.01

DMD Fast Forward. Published on November 4, 2019 as DOI: 10.1124/dmd.119.087940
This article has not been copyedited and formatted. The final version may differ from this version.

Figure 1.

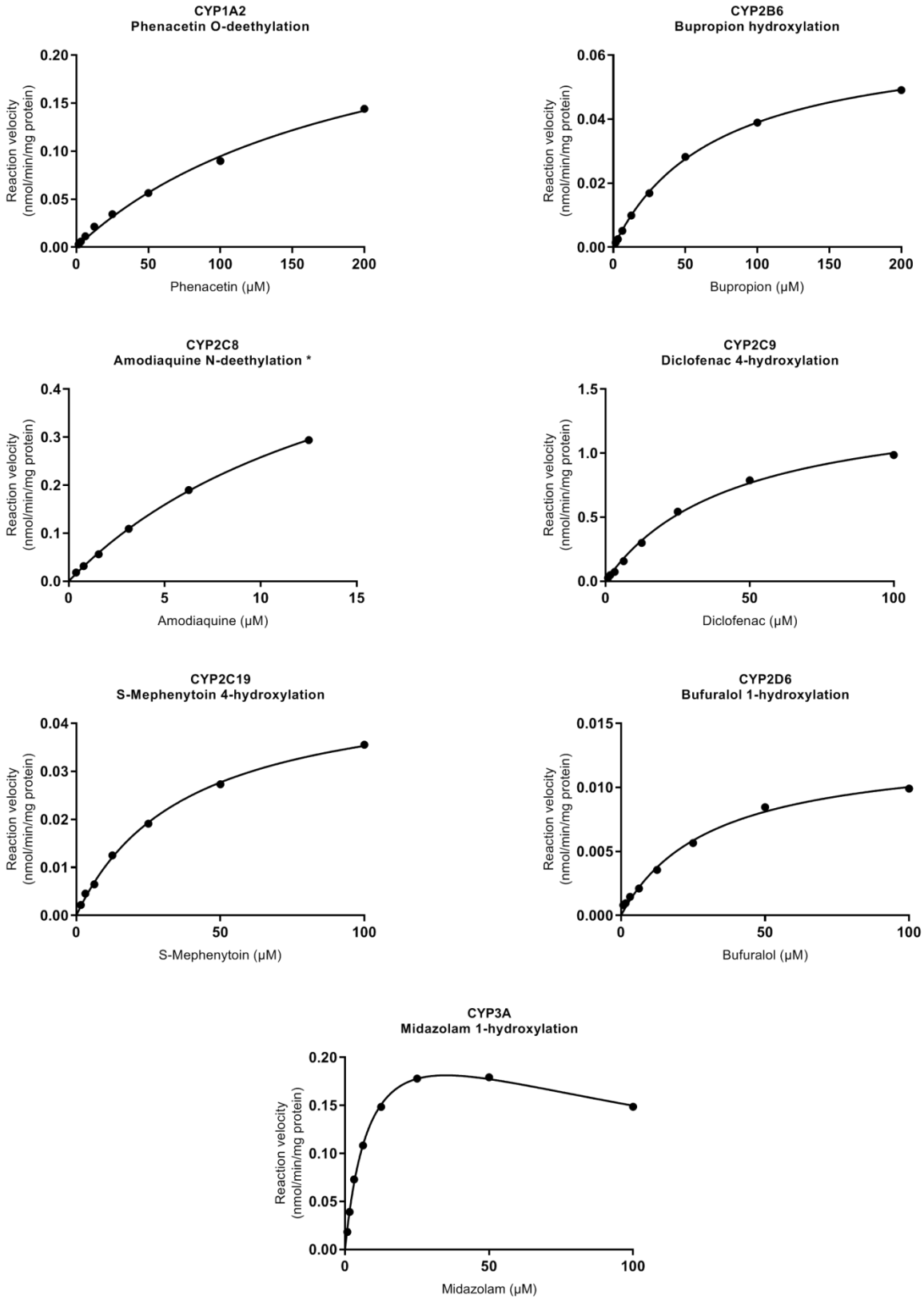

DMD Fast Forward. Published on November 4, 2019 as DOI: 10.1124/dmd.119.087940
This article has not been copyedited and formatted. The final version may differ from this version.

Figure 2.

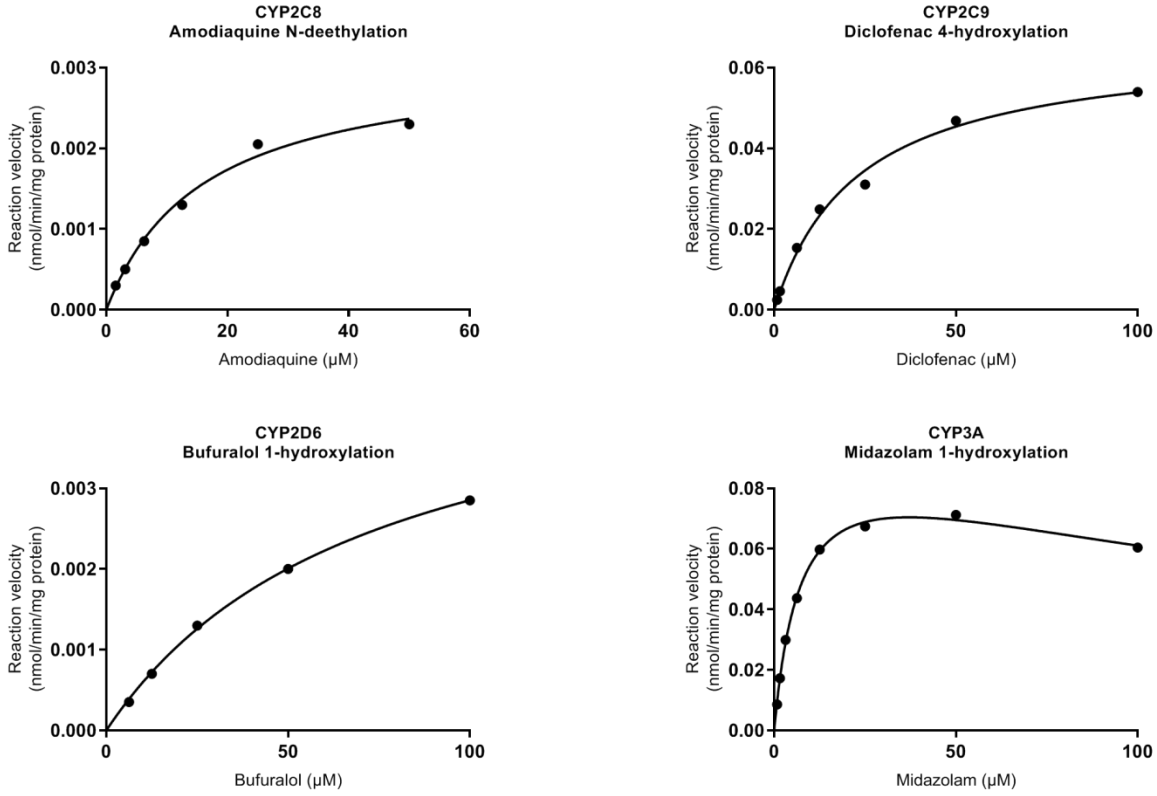

DMD Fast Forward. Published on November 4, 2019 as DOI: 10.1124/dmd.119.087940
This article has not been copyedited and formatted. The final version may differ from this version.

Figure 3.

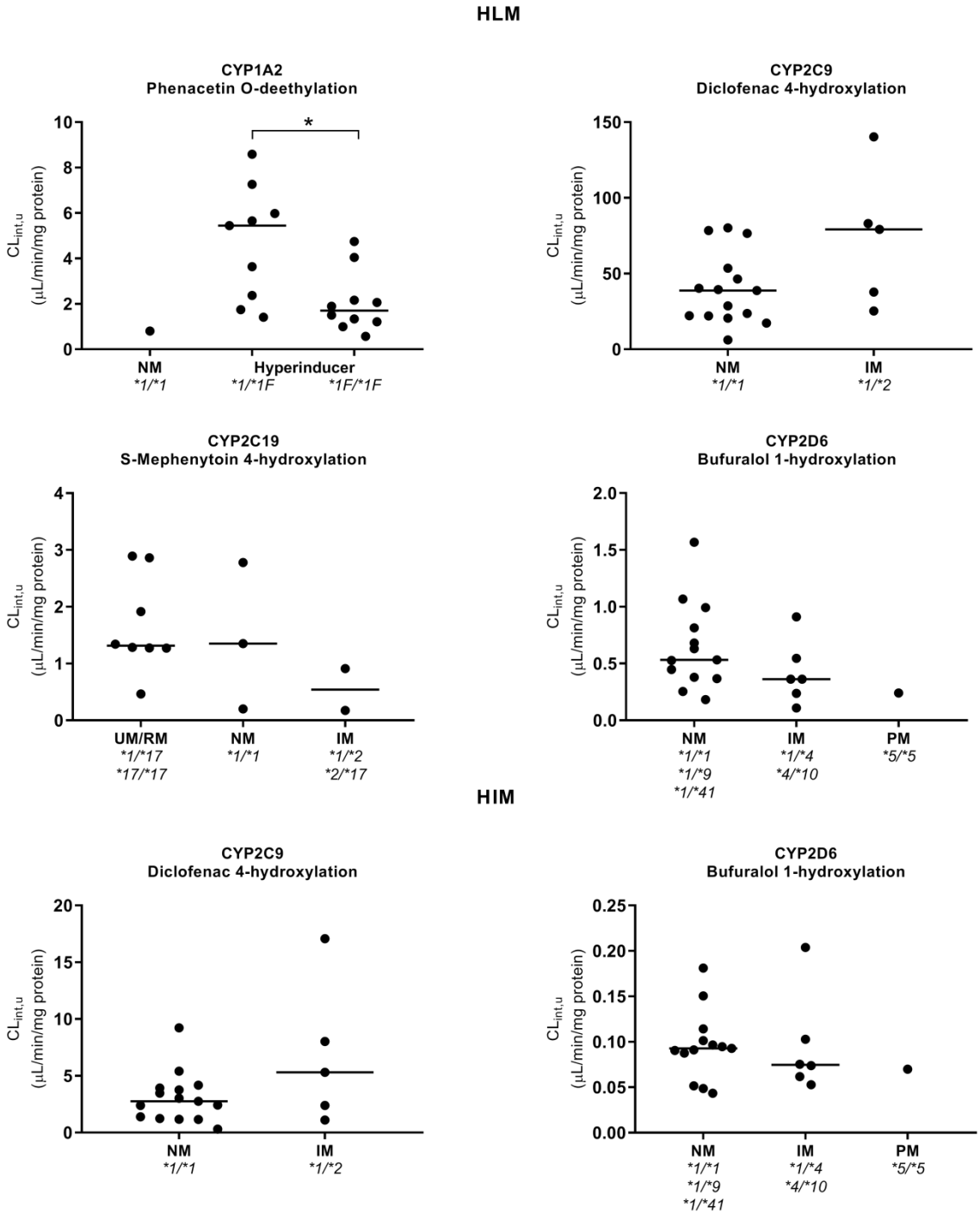

DMD Fast Forward. Published on November 4, 2019 as DOI: 10.1124/dmd.119.087940
This article has not been copyedited and formatted. The final version may differ from this version.

Figure 4.

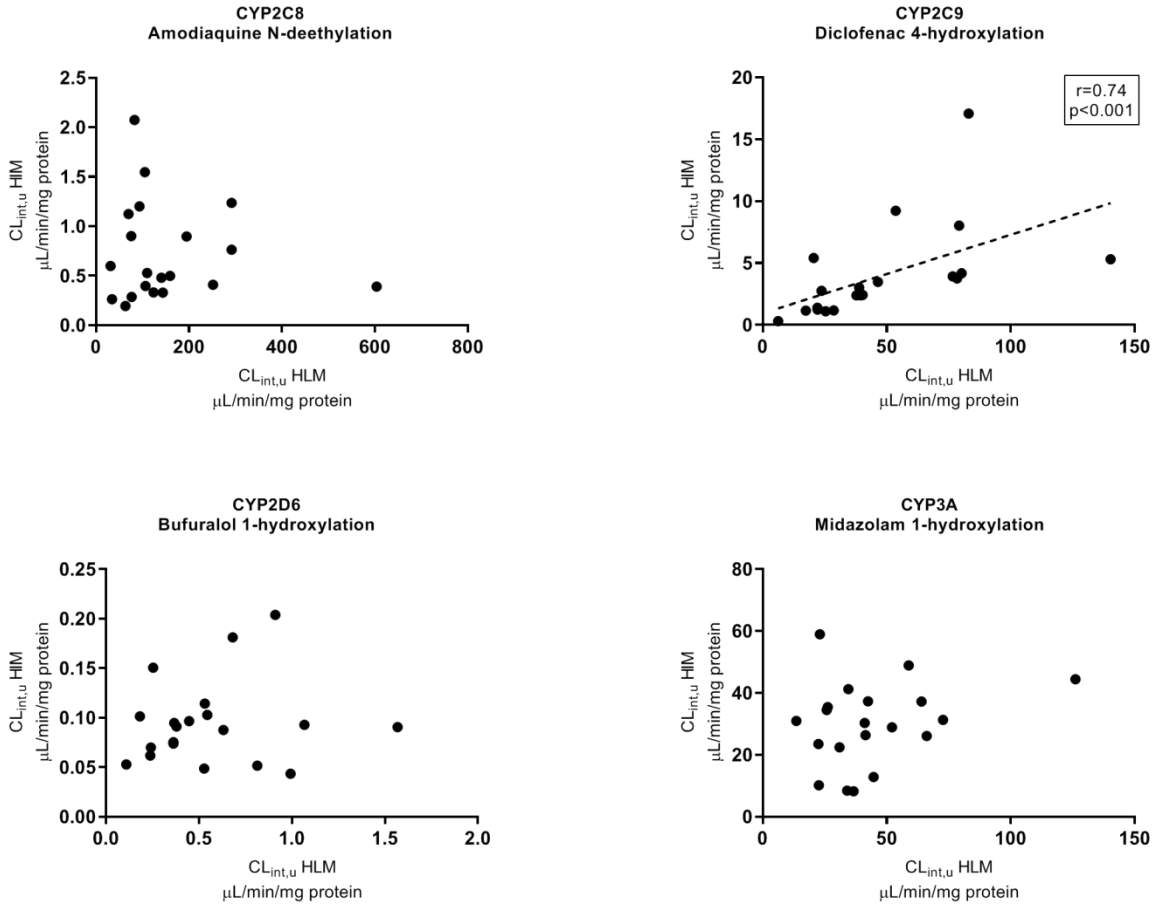

DMD Fast Forward. Published on November 4, 2019 as DOI: 10.1124/dmd.119.087940
This article has not been copyedited and formatted. The final version may differ from this version.

Figure 5.

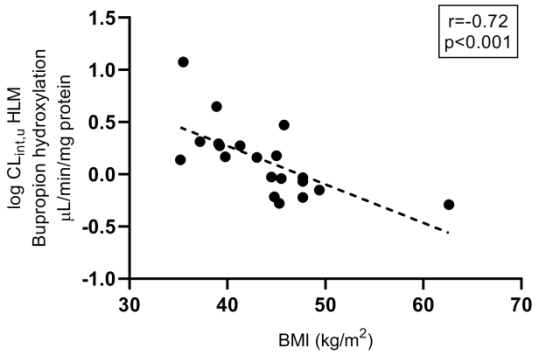

DMD Fast Forward. Published on November 4, 2019 as DOI: 10.1124/dmd.119.087940
This article has not been copyedited and formatted. The final version may differ from this version.

Figure 6.